Fuel 338 (2023) 127297

Contents lists available at ScienceDirect

Fuel

journal homepage: www.elsevier.com/locate/fuel

Full length article

Feedstock flexible numerical analysis of sewage sludge gasification

Corinna Netzer *, Ning Guo, Ivar Ståle Ertesvåg, Terese Løvås

Department of Energy and Process Engineering, Faculty of Engineering, Norwegian University of Science and Technology, Kolbjørn Hejes vei 1a, Trondheim, 7034, Trøndelag, Norway

ARTICLE INFO

Keywords:
Sewage sludge
Gasification
Detailed chemistry
Surrogate
Stochastic reactor model
NO_x and SO_x

ABSTRACT

Sewage sludge properties vary with the origin and treatment method of the wastewater. When converting the sewage sludge thermally for material and energy recovery, these properties affect the composition of the products and the efficiency of the process. Rotary kiln gasifiers can handle these variations in the raw materials. For further development, process integration, optimization of the process, upscaling, and industrial application, it is helpful to understand and describe the impact of the sewage sludge properties on operating parameters and product quality. This work analyses the impact of sewage sludge properties numerically using detailed chemistry and the surrogate approach. Sewage sludge is described using woody biomass components, sugars, lipids, proteins, inorganic species, moisture, and ash. The stochastic reactor model (SRM) is used to model the gasification process. In contrast to ideal reactors, stochastic reactors allow for resolving inhomogeneity. Hence, the predicted gas composition results from local temperature and available oxygen. For the analysis, temperature, airflow rate, and fuel properties, i.e., the amount and composition of volatiles, including fuel-bonded nitrogen and sulfur, and the moisture level are varied. Their results are analysed regarding the produced gas composition, emission precursor formation, and cold gas efficiency of the process. The highest efficiencies are found for temperatures of 1223 K and rich conditions. High concentrations of methane and hydrogen accompany this maximum. However, the producer gas's highest heating value is found at low temperatures thanks to the presence of small hydrocarbons. Furthermore, a high volatile amount and a dry feedstock favour methane and carbon monoxide formation. The hydrogen concentration is found to be sensitive to the moisture content and is the highest at 30%. The cold gas efficiency is predicted to depend strongly on the feedstock and varies for the same operating conditions up to 60%. With increasing fuel-bonded nitrogen and sulfur content, the concentrations of NO and SO_2 formation and their precursors increase, respectively. The released ammonia leads to significantly reducing emitted NO through the ThermalDeNOx mechanism. Overall, the generated maps provide a detailed insight in species formation and allows for the prediction of process parameters sensitive to the sewage sludge properties.

1. Introduction

Sewage sludge is a byproduct of wastewater treatment of municipalities and industry. Hence, its emergence will further increase with the world's population, and it will accumulate in metropolitan areas. Traditionally, sewage sludge has been used directly as fertilizer in agriculture or via composting, thanks to its high nitrogen and phosphorus contents. However, sewage sludge contains components hazardous to humans and the environment due to the wastewater's various origins. Harmful contaminants are, among other inorganic compounds, e.g., heavy metals [1–3] and organic substances, e.g., pesticides, pharmaceuticals [4,5]. To avoid the emission of harmful substances in the environment and recover the nutrition and energy content of the waste stream, thermal treatment processes can be employed. Thermal treatment allows sterilization of the sludge, increases the concentration of non-volatile species in the solid, and recovers the energy content. Under oxygen exclusion and oxygen-poor atmospheres, sewage sludge is converted to syngas, condensable species (tar), and a solid char-rich fraction [6,7]. The resulting syngas and liquid can be used for energy and heat supply or further upgraded in gas-to-liquid processes [6]. The decontaminated char serves as fertilizer or is further treated to recover phosphorus [8] and other inorganic components. All thermal treatment processes require additional heat input to the system. However, comparing incineration, pyrolysis and gasification, the latter two release fewer emissions (nitrogen and sulfur oxide and dioxins) [6,9]. Thus, sewage sludge pyrolysis and gasification are estimated to be more

* Corresponding author.
E-mail address: corinna.netzer@ntnu.no (C. Netzer).

https://doi.org/10.1016/j.fuel.2022.127297
Received 1 October 2022; Received in revised form 6 December 2022; Accepted 24 December 2022
Available online 4 January 2023

beneficial to implementable in the future circular economy and local energy supply [7].

Frequently, fluidized bed gasifiers are applied to valorize sewage sludge, and other bio-derived waste streams, e.g., [10–12]. Their use is beneficial since fluidized bed converters provide fast mixing of raw material and conversion atmosphere and hence provide good control of the thermochemical pathways [6]. To allow larger variations of the raw material properties, fixed bed gasifiers (downdrafts and updrafts) are investigated, e.g., [13–15]. However, in both methodologies, the high ash content of sewage sludge and its high elutriation rate of fine material are obstacles to continuous operations due to increased fluidized bed height, slagging, and clinker formation [16]. Thanks to their continuous rotational motion that provides mixing of the raw material and discharge of the char and ashes, rotary kilns offer a solution related to the high ash formation by sewage sludge [16]. Hence, rotary kiln gasifiers have been investigated in lab-scale, and pilot plants [6,9,16–19]. Furthermore, rotary kiln converters allow for the conversion of materials with little or no pre-treatment, tolerating large variations in fuel size and shape and heating value [6].

Numerical simulations can support further development towards large-scale industrial applications by exploring a wide range of operating conditions, plant design, and the impact of the properties of the raw materials. An estimation and insight on expected variations in product streams and their quality, including emission, helps to design upgrading units and evaluate their efficiency. Furthermore, the detailed knowledge of the product gas composition allows for estimating the emission formation in subsequent heat and power applications. These insights are needed to develop reliable and sustainable energy supply solutions and their integration into circular economy and energy clusters.

In order to use numerical simulations as a design tool, the modelling needs to have a predictive character. For the thermal treatment of sewage sludge, it is necessary to describe the variation in the feedstock and its effect on the process and the product stream. Considering this, detailed chemistry models paired with flexible surrogate models are employed in this work. Detailed chemistry models offer the mathematical description of the devolatilization, heterogeneous reactions and gas phase processes, such as the cracking of large molecules and their oxidation. Surrogate models allow for a flexible numerical representation of the feedstock. As a result, key characteristics of the feedstock, here sewage sludge, and its gasification products can be modelled [20]. The surrogate concept is state-of-the-art in liquid and gaseous fuel modelling. For example, Diesel and gasoline fuels that consist of hundreds of different species are represented by n-heptane, and n-heptane/iso-octane mixtures, respectively and natural gas is typically represented by pure methane. For solid feedstocks, the surrogate representation typically combines several species. The surrogate representation by Debiagi et al. [21] includes nine reference species, including moisture and ash, and allows for the description of around 500 biomass and waste fraction samples, such as woods, grass plants, algae, and food industry wastes. Further models in the literature describe the thermal conversion of the solid feedstock of coal [22], woody [23–25] and algae biomass [26], municipal solid waste [27] and sewage sludge [28]. The surrogate model for sewage sludge represents the solid feedstock using different protein species, lignocellulosic species, and species to release fuel-bonded nitrogen and sulfur [28]. With the set of 15 species, the ultimate composition of the sewage sludge samples and their moisture and ash content can be formulated in close agreement [28]. In combination with the gas phase mechanism, originally developed for municipal solid waste [27], the further fate of the released tar, gas-species and NO_x and SO_x can be modelled. In total, the chemical model consists of 15 surrogate species, 37 solid species, 41 devolatilization and heterogeneous reactions, 188 gas phase species and 3207 homogeneous gas phase reactions.

While such a detailed chemistry treatment is necessary to capture dependencies on the feedstock and emission formation, it is too large for efficient use in three-dimensional fluid dynamic simulations. On the other hand, ideal zero-dimensional reactors have the benefit of short simulations. However, they lack the detailed description of local variations of temperature, available oxygen and species concentrations that are essential for emission prediction. As a compromise between the two types of simulations, the stochastic reactor model has been developed (introduced for solid fuel conversion in [29,30]), combining the benefits of both. The zero-dimensional character of the models allows to solve detailed chemistry schemes efficiently, and the discretization of the reactor domain into dimensional "packages" or "particles" enable to resolve the distribution functions within the reactor domain. Stochastic reactor models can be used to calculate operating conditions maps with low computation cost and provide the needed sensitivity towards local temperature and species concentration for predicting species and gas phase emissions.

This work aims to model and analyse the impact of the fuel properties (moisture content, volatile content, and ultimate composition) on the expected product gas composition and cold gas efficiency of the process. Moreover, the concentration of nitrogen and sulfur species is analysed for various fuel samples and operating conditions to estimate the potential of NO_x and SO_x formation in a consecutive incineration stage. For the analysis, the surrogate approach and detailed chemistry models for sewage sludge [27,28] are applied together with the stochastic reactor model [29,30]. The models are applied and compared to a rotary kiln experimental setup from literature [16].

The highlight of the presented study is the flexible representation of sewage sludge in numerical simulations, which allows considering its properties in simulations. Producer gas species and efficiency maps are calculated for a matrix of temperatures and air–fuel equivalence ratios, and 17 analysed sewage sludge samples and five moisture contents. The devolatilization of nitrogen and sulfur species is modelled, and the dependencies of NO_x and SO_x formation in the producer gas is analysed.

The paper is structured as follows: first, the used chemistry, the stochastic reactor model approach and the experimental setup are introduced. The following results section presents the model's validation against the experiment, the impact of temperature and equivalence ratio on the cold gas efficiency (CGE), followed by the impact of the feedstock on product quality and CGE, and last, the formation of NO_x and SO_x precursors for all operating conditions. In the end, several important conclusions are summarized.

2. Methodology

2.1. Chemical model

The chemical model consists of three parts: a set of surrogate species to describe sewage sludge mathematically [28], a multistep reaction scheme including devolatilization reactions and heterogeneous reactions of gas-phase and char [28], and a description of the gas phase using detailed kinetics [27].

The elemental and macro-molecular composition of sewage sludge varies widely: the volatile content lies between 40 and 60 wt% of the dry matter (including ash) [28,31] consisting of lignocellulosic compounds (~ 30 wt% lignins, ~ 10 wt% cellulose, < 5 wt% hemicellulose [2]), proteins (18–40 wt% [2]), sugars, oil, grease, and others [2,32]. Based on these commonly found components, surrogate species have been selected for the numerical representation of sewage sludge. The surrogate species are adopted from wood [24], algae biomass [33], and municipal solid waste [27]. Herein, protein species enable to model the release of fuel-NO precursors. Furthermore, species to account for gas release by inorganic components model the release of sulfur species and further release of ammonia and carbon dioxide [27]. All surrogate species and their elementary composition are listed in Table 1. Surrogates are formulated using sewage samples' ultimate composition, ash, and moisture content as the target for a linear least-squares fit.

Table 1
Surrogate species for the representation of sewage sludge [28].

Surrogate species	Representation	Elementary composition					
		C	H	O	N	S	Si
CELL	Cellulose	6	10	5	0	0	0
HCE	Hemicellulose	5	8	4	0	0	0
LIG_C	Lignin rich in C	15	14	4	0	0	0
LIG_H	Lignin rich in H	22	28	9	0	0	0
LIG_O	Lignin rich in O	20	22	10	0	0	0
SUGAR	Monosaccharide	6	8	6	0	0	0
LIPID	Lipids	18	32	2	0	0	0
$PROT_H$	Protein rich in H	400	900	150	86	0	0
$PROT_C$	Protein rich in C	500	450	65	80	0	0
$PROT_O$	Protein rich in O	250	500	200	72	0	0
NH_3I	Product gas inorganic nitrogen	0	3	0	1	0	0
CO_2I	Product gas inorganic carbon	1	0	2	0	0	0
(H_2S SO_2 COS)I	Product gas inorganic sulfur	1	2	3	0	3	0
H_2O(S)	Moisture content	0	2	1	0	0	0
ASH	Ash content	0	0	0	0	0	1

As additional constraints, fixed ratios of the lignocellulosic compounds are set [21,34].

The corresponding reaction scheme consists of apparent reactions in Arrhenius formulation with up to four intermediate steps. Hereby, the surrogates are stepwise decomposed, yielding partially decomposed solid species, char, tar and gas species tar. Tar species include molecules up to C_{11}, single and double aromatics, and nitrogen-containing cyclic species [27].

Detailed decomposition reactions describe their break-up under thermal stress with and without available oxidizers and their interaction with other gaseous species. This complex description allows modelling their breakdown to small hydrocarbons and products, such as CO_2, CO, H_2, H_2O, and others, sensitive to local conditions. This capability is needed for predicting the amount and speciation of the product gas and tar yields sensitive to the feedstock, local temperature, available oxidizers, and radical pool. This flexibility is essential, especially at low airflow rates that limit the oxidation of the tar and gas species, e.g., in the transition regime from pyrolysis to gasification, and for the analysis of different gasification agents, such as air and steam. The zero-dimensional model framework enables treating the gas phase chemistry in detail, typically only resolved in ideal reactors. The combination of the resolution of the temperature and species space (Section 2.2) and the detailed reaction mechanism allows moving towards predicting simulations and analysing the gas and tar species dependent on the feedstock and local conditions in the reactor. For emission prediction, the nitrogen and sulfur chemistry by Glarborg and coworkers are included [35–37]. The scheme includes fuel-, thermal- and prompt-NO pathways, and reactions for the oxidation of sulfur species and their interaction with nitrogen oxides. The mechanism consists of 188 gas-phase species and 3207 reactions [27].

2.2. Numerical model

The stochastic gasification model available in LOGEreserach version 1.10 [29] is applied for all simulations. It allows for resolving devolatilization, heterogeneous reactions of solid and gas phases, and homogeneous reactions in the gas phase. The model is formulated in a zero-dimensional framework using the Probability Density Function (PDF) approach, and the reactor volume is discretized using stochastic non-dimensional particles. Each particle is described by the content of three phases (the solid phase, the pore gas in the solid and the laminar boundary layer, and the bulk gas), its energy content, and the species compositions of the three phases (Fig. 1). Each stochastic particle undergoes an individual temperature history over the simulation time. The temperature of a stochastic particle can change by heat transfer with the hot reactor wall, radiation, mixing of the bulk gas phase with another stochastic particle, and chemical reactions [29,30]. The selection of particles for heat transfer and mixing is stochastic. The mixing step can increase or decrease the available oxidizer in one stochastic particle or exchange highly reactive species, such as radicals, from one stochastic particle to another. The local temperature and available gas phase species affect the local reactions and hence species pool and vice versa. Hence, during the simulation, the distribution of bulk gas, pore gas, and solid phase temperature and of the species in each phase over all stochastic particles are resolved. Due to the zero-dimensional character of the model, the physical space is not resolved; however, the temperature and species space are resolved and represent the inhomogeneous fields within a pyrolysis or gasification device. This inhomogeneous temperature and species profile is a typical characteristic of stochastic reactor models and allows, opposite to ideal reactors, their use for the analysis of local phenomena, such as species decomposition and emission formation [38]. For the stochastic gasification model, this capability has been demonstrated within the analysis of species, and temperature distributions in each gasification reactor and the fuel bed of a grate-fired incineration plant [39].

The calculation of the devolatilization rates and heterogeneous reactions provides source terms for the gas phase and is used to model the consumption of the solid. The further decomposition and oxidation of the released gas and tar species are predicted based on a detailed gas-phase mechanism [29,30].

Heat and mass transfer are modelled by the mixing of the bulk gas and interaction between the two gas phases. In the model, the pore gas exchanges heat and mass with the bulk gas determined by Nusselt and Sherwood laws [29,30]. In the mixing step, only the bulk gas (species and enthalpy) is mixed with another particle and mimics the convective mass transport and the associated heat transfer. Further, radiation between the reactor wall and particles is calculated according to the Stefan–Boltzmann law, using the emissivity and temperatures of both phases [29,30].

The stochastic mixing of the bulk gas between stochastic particles models the turbulence of the gas phase and is determined by the mixing time. Low mixing processes, such as grate-fired and fixed bed applications, are represented using one mixing event per numerical time step, i.e., a scalar mixing time τ_{mix} of 1 s [39]. For example, a highly turbulent flow, present in entrainment flow gasifiers, is modelled using mixing times between 0.001 to 0.05 s [29,39].

The here applied stochastic gasification model can be used in different configurations: as a series of partially stirred reactors with one gas and fuel inlet in the first reactor, a partially stirred plug flow reactor, or connected to a reactor network model with multiple gas and solid stream inlets [29,30,39]. Depending on the provided chemical model and operating conditions, such as air feed rare and heat transfer from the boundaries, it allows to model pyrolysis, gasification, and combustion applications [27,30,39].

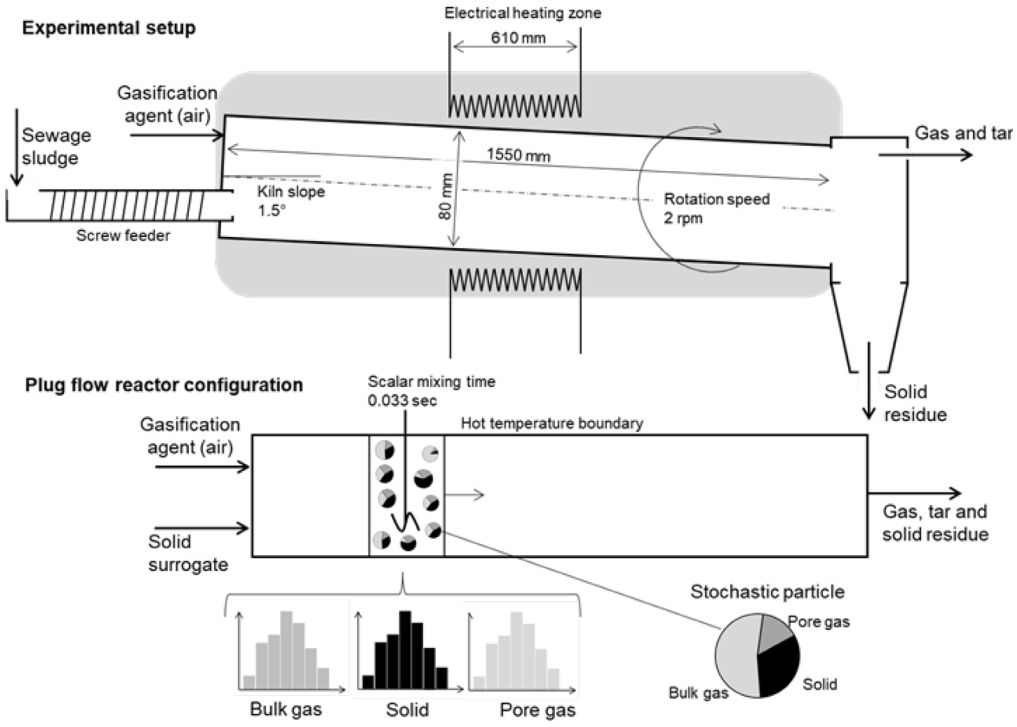

Fig. 1. Illustration of the experimental setup by Freda et al. [16] (top) and its numerical representation using the stochastic reactor model in plug flow configuration (bottom).

2.3. Numerical setup

The presented analysis is based on the experimental results of Freda et al. [16]. They performed measurements of the thermal treatment of partially dried sewage sludge for pyrolysis and gasification conditions. The sewage sludge is converted using a bench-scale rotary kiln gasifier employing air as the gasification agent. The kiln is illustrated in Fig. 1. The kiln has a total length of 1550 mm and an inner diameter of 80 mm. The heat for gasification is provided electrically over a length of 610 mm. Freda et al. [16] studied different operating conditions. For the presented numerical analysis, the gasification condition with the highest achieved cold gas efficiency is chosen: a temperature of 1123 K, an air–fuel equivalence ratio $\lambda = 0.16$ with a solid feedstock feed of 237 g/h and the air flow rate with 3 Nl/min. For these conditions, the rotary kiln yields a dry produced gas with a lower heating value (LHV) of 7.9 MJ/Nm^3_{dry} and a cold gas efficiency (CGE) of 67% in the experiment [16]. Overall, those authors concluded that the apparatus yields a relatively clean, dry producer gas consisting mainly of CO, H_2, CH_4, and CO_2.

The stochastic reactor model is run in a plug flow configuration (Fig. 1) to replicate the rotary kiln gasifier. The sewage sludge surrogate and corresponding air flow rate are fed to the reactor inlet. The mixing time, an optimization parameter, is set to 0.033 s. This value corresponds to the kiln rotational speed of 2 rpm and classifies the mixing as low compared to other applications, as discussed above. The sewage sludge sample analysed by Freda et al. [16] is reproduced using the above-introduced surrogate species and the linear-least square method. The authors further state that the sewage sludge had to be partially dried to prevent the rotary kiln from clogging in the experiment [16]. In the present simulation study, a moisture content of 20 wt% is found to be most plausible during the model calibration. This surrogate is in the following, denoted with the ID 0. Other surrogates ("1" to "17") based on the experiments by Gomez-Rico et al. [31] are formulated to analyse the impact of various sewage sludge samples. All employed sewage sludge surrogates are compared to their ultimate composition of the sample in Table 2. Their formulation is further discussed in [28] and here reported for the readability of the paper. The speciation of the surrogates is further shown in Fig. 2.

The presented study aims to analyse the cold gas efficiency (CGE), defined as

$$CGE = \frac{LHV_{gas} \times gas\ yield}{LHV_{solid}}. \quad (1)$$

where the lower heating value of the gases is calculated in MJ/m^3 of dry producer gas, the gas yield is given as m^3 dry gas per kilo solid feedstock, and the lower heating value of the solid in MJ/kg. Moreover, the producer gas composition over a variation in operating conditions (temperature and equivalence ratio) and feedstock (sewage sludge surrogates and moisture content) is investigated. The experimental condition (T = 1123 K, $\lambda = 0.16$), as described above, serves as the base case since it has the highest CGE in the experiments. The simulation matrix for the operating conditions is set to:

- Wall temperature: 923 to 1223 K in 50 K steps;
- Air–fuel equivalence ratio λ: 0.1 to 0.4 in 0.025 steps.

And the feedstock variation matrix is set to:

- Feedstock: surrogate 1 to 17 (Table 2 and Fig. 2);
- Moisture content (mass%): 10 to 50% in 10% steps.

The hot temperature boundary is set to the aimed ambient temperature 1123 K for the temperature variation. The airflow is adjusted to adjust the equivalence ratio to the desired ratio of solid feedstock and air, while the solid feedstock remains in all simulations constant (237 g/h). For the variation of the sewage sludge surrogate, the solid feed boundary is replaced by the surrogate specifications from Fig. 2. The shown compositions are linearly mixed with the surrogate species H_2O(S) to mimic variations in moisture content. Also, for these variations, the fuel boundary mass flow is the same for all simulations. Due to the differences in lower heating values (LHV), ultimate composition and ash content of the surrogates, the constant mass flow leads to variations in the energy flow into the system and slight variations in the element-based equivalence ratio, here in terms of amount and composition of the volatile matter versus gasification air. This shift

Table 2
Ultimate composition analysis (UCA) of sewage sludge samples reported by Freda et al. [16] (ID 0) and by Gomez-Rico et al. [31] (ID 1 – 17) and their surrogate representation [28]. Values denote mass percentages in the dry fuel, including ash. The oxygen mass concentration is given by difference. Lower heating values (LHV) are calculated using the correlation of Channiwala and Parikh [40].

ID	UCA measurement					Surrogate representation					
	C (wt%)	H (wt%)	N (wt%)	S (wt%)	Ash (wt%)	C (wt%)	H (wt%)	N (wt%)	S (wt%)	Ash (wt%)	HV MJ/kg
0	41.2	5.22	3.21	–	29.7	40.9	5.22	3.21	–	29.7	16.5
1	41.2	6.10	3.60	0.83	24.0	40.8	5.75	3.70	0.80	24.0	17.9
2	25.1	3.90	2.70	2.50	40.0	25.1	3.90	2.70	2.50	40.0	12.4
3	40.8	6.10	3.10	0.71	27.0	40.3	5.48	3.28	0.66	27.0	18.9
4	38.5	6.00	3.90	1.20	26.0	38.2	5.65	4.00	1.17	26.0	16.7
5	35.3	5.10	2.90	0.90	36.0	34.9	4.80	2.98	0.88	36.0	18.5
6	31.1	4.10	1.90	0.71	40.0	30.8	4.11	1.90	0.71	40.0	17.6
7	37.3	5.70	3.60	1.30	30.0	36.9	5.32	3.70	1.27	30.0	17.3
8	29.3	4.30	2.50	0.56	37.0	29.2	4.31	2.50	0.56	37.0	14.6
9	42.0	6.30	4.40	1.50	25.0	41.4	5.73	4.45	1.32	25.0	17.9
10	35.9	5.50	6.20	4.20	30.0	35.7	5.41	6.21	4.17	30.0	14.3
11	40.5	5.90	2.10	0.52	21.0	40.2	5.52	2.21	0.49	21.0	17.8
12	28.5	4.70	4.60	1.50	37.0	28.4	4.70	4.60	1.50	37.0	12.1
13	32.0	4.60	2.10	0.69	38.0	31.7	4.43	2.15	0.68	38.0	17.6
14	26.3	4.20	3.40	1.20	44.0	26.2	4.20	3.40	1.20	44.0	13.9
15	19.8	2.80	2.10	2.80	55.0	19.7	2.80	2.10	2.80	55.0	13.2
16	24.8	3.90	3.20	1.30	49.0	24.7	3.90	3.20	1.30	49.0	14.7
17	24.4	3.40	1.90	0.78	54.0	24.1	3.36	1.91	0.78	54.0	17.9

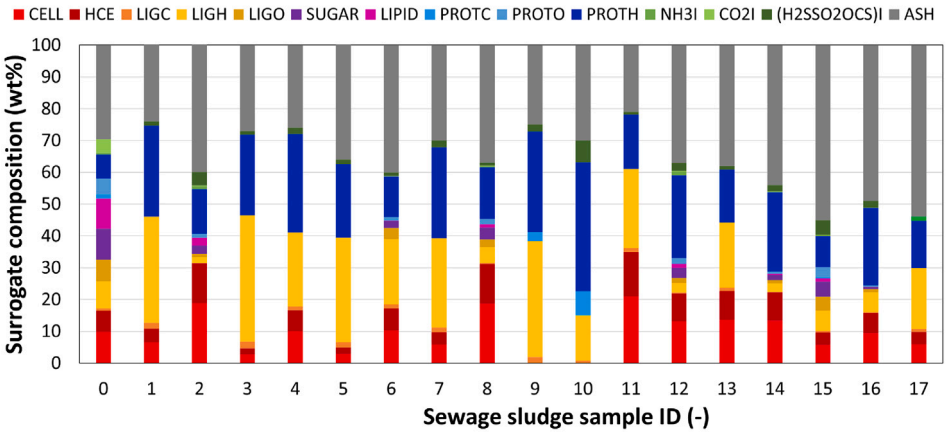

Fig. 2. Composition of the surrogates corresponding to Table 2.

in equivalence ratio increases with simulated moisture content since the corresponding mass (volatiles and ash) are replaced by the water content.

3. Results and discussion

3.1. Validation of the modelling approach

The experiment by Freda et al. [16] is reproduced using the sewage sludge sample "0" for model validation. The predicted yield of the different product fractions, lower heating value (LHV) of the product gas, and the cold gas efficiency (CGE) are shown in Fig. 3 and from the experiment available species concentrations in Fig. 4. For this comparison, all species with a molar mass larger than benzene are collected to calculate the tar yield. The model captures the distribution of the different product fractions (char, gas, tar, and water). The tar yield is overpredicted. The higher predicted tar mass leads to slight underprediction of the main gas-phase products (carbon dioxide CO_2, carbon monoxide CO, hydrogen H_2, and methane CH_4). In the simulation, tar is not further decomposed due to a lack of available oxygen. The gas yield, LHV, and cold gas efficiency are considered well reproduced. The concentrations of the main gas products and other small hydrocarbons, ethane C_2H_6 and propane C_3H_8 (no formation in the experiment, < 1 ppm in the simulation) are well predicted. The model's capability to reproduce trends in varying gasification agents and temperature for this specific apparatus has been demonstrated as part of the reaction mechanism development [28] and hence not further discussed here. The here shown prediction and previous validation allow using the numerical setup for the aimed numerical study towards the impact of fuel properties on gas quality and process efficiency.

3.2. Impact of operational parameters

The results for gas yield, lower heating value (LHV) of the dry producer gas, and the cold gas efficiency (CGE) of the process for the temperature and airflow rate (air–fuel equivalence ratio) are shown in Fig. 5. The air–fuel equivalence ratio is calculated here based on the elements rather than the fuel and oxidizer mass flows. In this way, oxygen atoms bonded in the surrogate species are also accounted for their oxidation capacity.

The simulated process produces more gas with increasing temperature and available oxygen. This result is consistent with the experimental findings by Freda et al. [16] and the phenomenological knowledge of the gasification process, where higher temperatures and higher available oxidizers lead to increased char and tar conversion. Both processes lead to a higher gas formation. In Fig. 6, it can be seen that

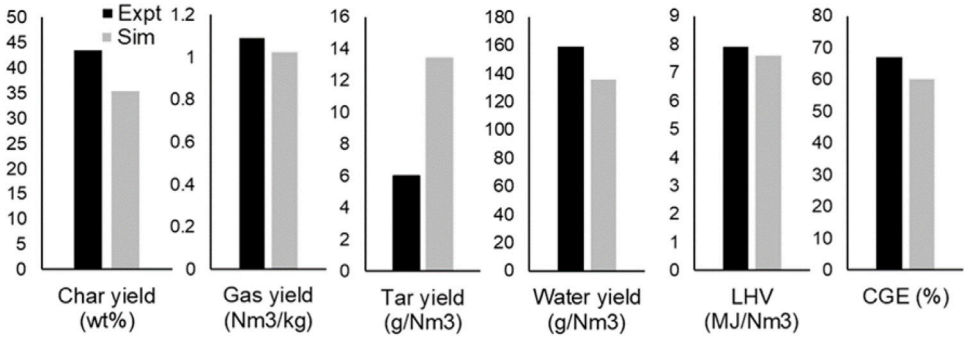

Fig. 3. Prediction of process characteristics at 1123 K and $\lambda = 0.16$. If applicable, values refer to the dry gas at normal conditions. *Source:* Experimental results from Freda et al. [16].

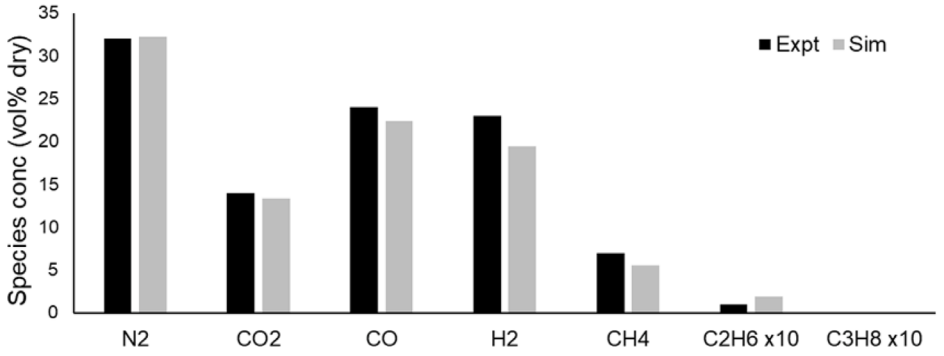

Fig. 4. Prediction of species concentrations at 1123 K and $\lambda = 0.16$. *Source:* Experimental results from Freda et al. [16].

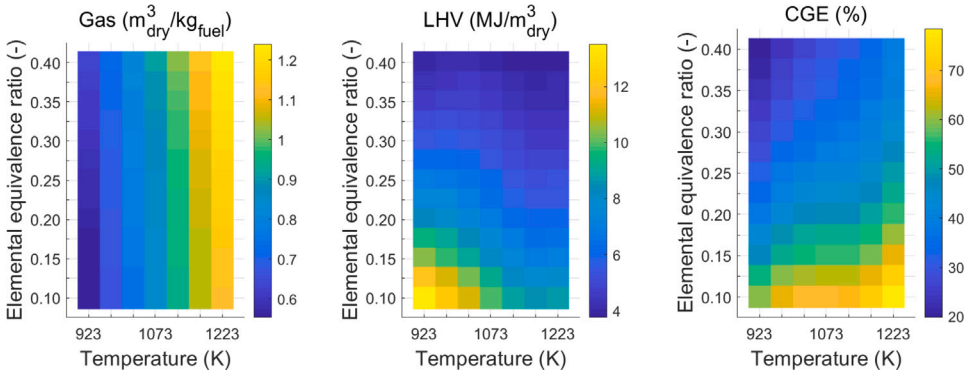

Fig. 5. Prediction of amount and energetic quality over the analysed fuel–air ratios and ambient temperatures.

this increased gas formation is largely due to the formation of carbon dioxide CO_2 as the product of char oxidation and other gasification end products, such as methane and hydrogen that result from the further decomposition of hydrocarbons. The lower heating value of the producer gas has a maximum at the lower temperature range and the lowest analysed equivalence ratio (Fig. 5). This maximum is co-located with the maximum of CO and hydrocarbons in the range of C_2 to C_6. In Fig. 6, ethane C_2H_6 is shown exemplary. The high concentrations of hydrocarbons (C_2 to C_6) increase the heating value significantly. The decrease of the heating value with increasing temperature and air supply aligns with measurements [16].

The CGE, which is a combination of the amount of produced gas, its lower heating value and the energy content of the feedstock, increases with temperature for all analysed airflow rates. This increase is mainly attributed to the increase in produced gas. The maximum CGE is accompanied by the maximum concentrations of methane and hydrogen. With increasing temperature and hence electric energy input, the larger hydrocarbons get further decomposed, and CO is converted to CO_2. The additional oxygen origins from fuel-bonded oxygen freed during further decomposition of oxygenated hydrocarbons and from the dissociation of water. The dissociation of water also allows a higher formation of hydrogen at high temperatures. Fig. 6 also shows the wet volume concentration of water. The significant decrease of water concentration with increasing temperatures and equivalence ratios are caused by the thermal dissociation and by dilution of the mixture with increasing gas production, e.g. due to the increasing concentration of CO_2. For 1223 K and $\lambda = 0.1$, a CGE > 75% is predicted. This high efficiency is mainly caused by the increased hydrogen production and the energy input via the electric heating system, which is not considered during the CGE calculation. In summary, the model well predicts the trends with increased temperature and air feed rate. The use of the detailed chemistry approach allows an understanding of the conversion behaviour of the released hydrocarbons. The maps allow

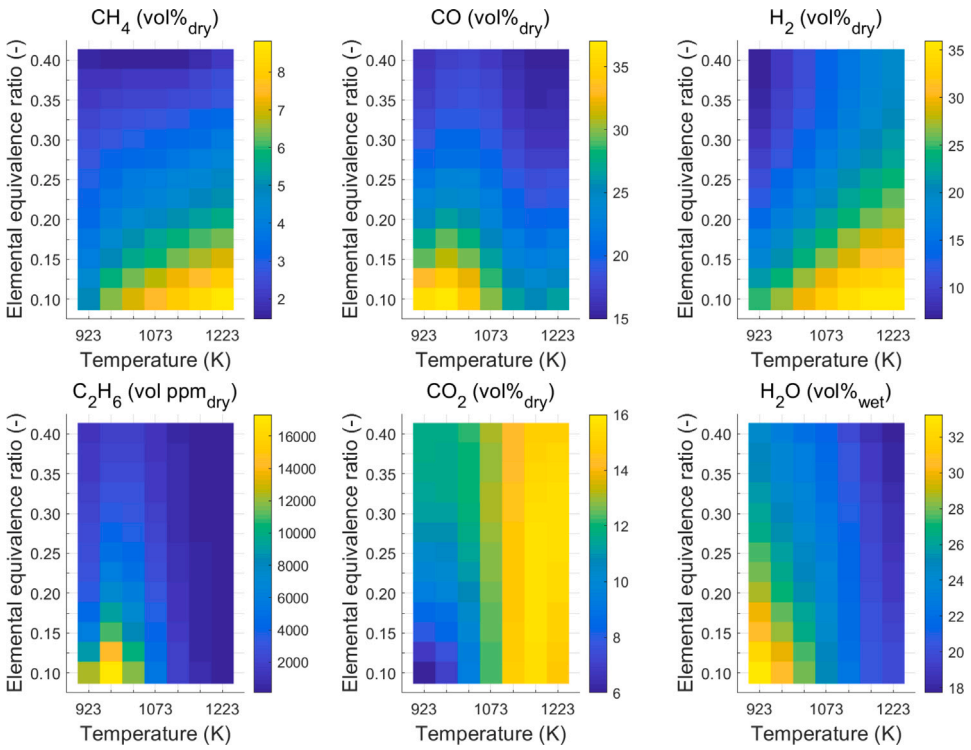

Fig. 6. Prediction of main gas components over the analysed fuel–air ratios and ambient temperatures.

finding the optimum in lower heating value, species concentrations and CGE for the targeted further use of the producer gas.

3.3. Impact of fuel properties

The same operating conditions are calculated for all sludge samples reported in Table 2. The dry ash-including surrogates (Fig. 2) are linearly combined with the surrogate species $H_2O(S)$ to achieve surrogates with moisture contents between 10 and 50 wt%. The mass flow rate of the solid feedstock and the airflow rate are kept constant for the simulation of the different samples. The constant solid mass flow leads due to the different heating values of the sewage sludge samples to a variation in the volatile and energy content. The different surrogates have further small variations in the stoichiometric air demand due to the variation in the fuel-bonded oxygen and total volatile amount. These variations in the surrogates lead to slight variations in the elemental air–fuel equivalence ratio and have to be considered during the interpretation of the results. The resulting differences of the product gas are the core of this analysis. The predicted concentrations of the main species in the produced dry gas, the corresponding lower heating value, and the gained cold gas efficiency are shown in Figs. 7 and 8. For these figures, the surrogates are ordered descendingly after the carbon content in the dry ash-including surrogate. The carbon content in the dry ash-including surrogate, also correlates with the amount of volatile matter.

The predicted maximum concentrations of methane (CH_4) and carbon monoxide (CO) are found for the sewage sludge surrogate with the highest carbon content in the dry ash-including surrogate (Fig. 7). From this maximum, the concentrations decrease with lower carbon content and volatile matter over the surrogate samples and moisture content. In the presented study, the moisture is added to the dry ash-including surrogate; hence, the volatile matter is reduced with increasing moisture content. The reduction of volatile matter with changing surrogate and moisture content enhances the formation of carbon dioxide CO_2 (Fig. 7). The surrogates with ID 15 to 17 are characterized by low carbon and high ash content. Hence, the stoichiometric air demand per kilogram sewage sludge surrogate is lower. This leads to a shift in the element-based equivalence ratio to leaner conditions. As a result, more carbon is fully oxidized. The same shift in equivalence ratio is caused by adding moisture content at constant surrogate inflow; hence, more CO_2 is formed with increasing moisture content. Moreover, with increasing moisture content, more water is dissociated at these high operating temperatures. This dissociation provides additional oxidizer to the system and is accompanied by an increase in hydrogen formation (Fig. 7). However, the hydrogen concentrations first increase slightly until 30wt% moisture and decline for higher moisture contents. The hydrogen formation is affected by the available water, but also by the decreasing volatile amount and hence fuel-bonded hydrogen. The predicted species trends in Fig. 7 agree with the measurement of similar processes reported by Chun et al. [19], and Xiong et al. [41].

The differences in species concentrations for the different sewage sludge samples also affect the amount of produced gas, its heating value and hence the cold gas efficiency of the gasifier. As shown in Fig. 8, with high carbon and volatile content (surrogates 9, 1, 3, 11) the highest gas production is predicted for the dry surrogate (10% moisture). This gas release is accompanied by a high lower heating value that is caused by the maximum concentrations of methane, other small hydrocarbons and carbon monoxide CO. The fuel properties (low carbon and low volatile content) that lead to the maximum CO_2 formation result in the lowest gas release and heating value. The maximum cold gas efficiency is found at the maxima of gas production and LHV. Furthermore, high efficiencies are also found for increasing moisture contents caused by the increase in hydrogen formation. Surrogates 9, 1, 3, 11 and 4 have higher volatile contents than the sewage sludge analysed in the experiments, denoted with 0 in Table 2. This leads to the prediction of CGE > 80%. On the lower end, for surrogates with low volatile contents and a high moisture content CGE ≈ 30% is calculated. This is caused by the lower amount of energy-containing matter and the high energy demand of drying.

The significant variation in sewage sludge properties is well known and considered one of the challenges in the operation of sewage sludge gasification. The presented analysis shows that the flexible surrogate

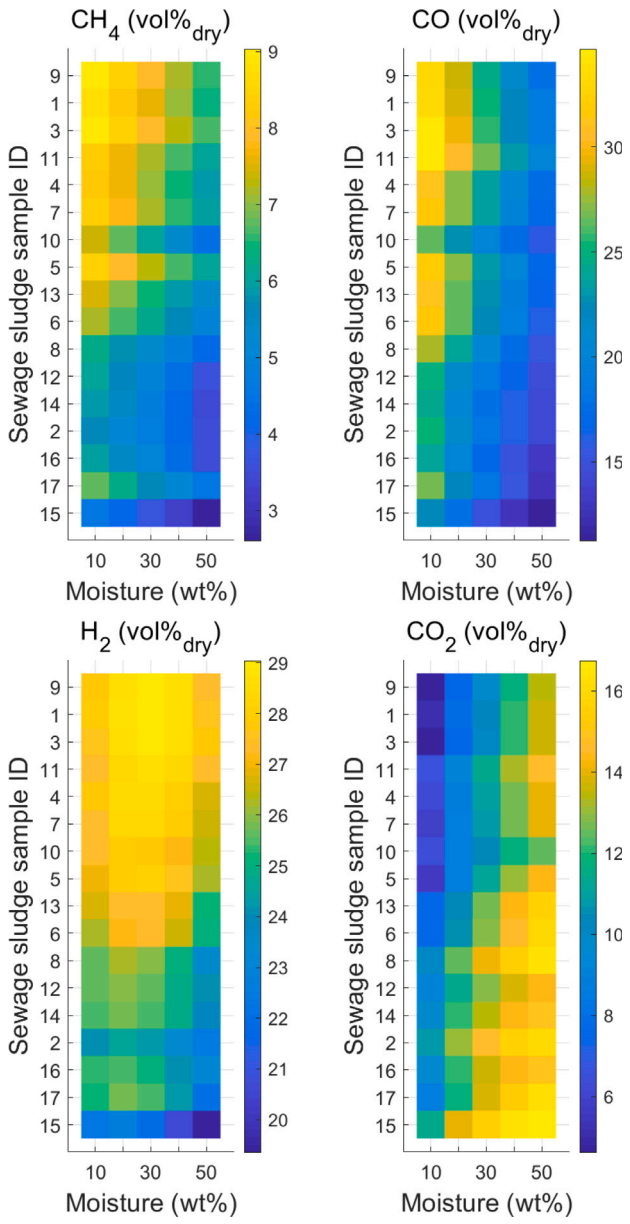

Fig. 7. Prediction of main gas components over the analysed surrogate compositions and moisture contents. Surrogate samples in descending order after carbon content in the dry ash including surrogate.

formulation based on the properties of the feedstock reproduces variations in the producer gas composition. With this, the results are sensitive to fuel properties (amount of fuel bonded elements, ash content and moisture content) and related changes in the equivalence ratio and oxidizing atmosphere (water concentrations). As a result, the change in producer gas amount and quality is predicted. The variation in CGE of 40 to 90% is significant. However, considering the difference in the lower heating value of the analysed sewage sludge samples this difference is plausible. Based on the presented results, a techno-economical or exergy analysis of the system can be carried out. This information is essential for the design process of a gasification plant and will be part of future work.

3.4. Gas phase emissions

The detailed formulation based on the ultimate component analysis allows studying the release of nitrogen oxides NO_x and sulfur oxides SO_x for the analysed conditions. In the employed model, fuel-bonded nitrogen is released in the form of ammonia NH_3, hydrogen cyanide HCN, as nitrogen-containing tar species (pyridine and pyrrole) and directly as nitrogen oxide. Depending on the operating conditions (available oxidizer and temperature), the tar species are further decomposed to form small hydrocarbons, NH_3 and HCN. The commonly known fuel-NO precursors NH_3 and HCN contain the largest amount of the released nitrogen during devolatilization. Ammonia has a key role in fuel-NO formation since it acts as NO precursor, but also as a reduction agent [42–44]. Ammonia's ability to reduce NO is used in the ThermalDeNO$_x$ applications [42,45]. The double role of NH_3 can be observed in Fig. 9. This figure shows the release of NO and its precursors over the analysed temperature and equivalence ratio matrix. HCN, as a species directly released from the solid matter and a decomposition product, is primarily formed under rich conditions. With higher temperatures and further devolatilization of the char and decomposition of the nitrogen-containing tar, the concentration increases with temperature. With leaner conditions, HCN gradually oxidizes and forms NO and other products. The concentration of ammonia has its maximum under rich conditions and low temperatures. NO has a significant high formation at the lowest temperature, and low predicted concentrations at the higher temperature range. The significant differences in NH_3 and HCN behaviour and the maximum NO concentration at low temperatures are connected via the ThermalDeNO$_x$ mechanism. ThermalDeNO$_x$ mechanism is used in selective non-catalytic reduction for flue gas cleaning. For this NH_3 is injected into the flue gas where it reduces NO with the global reaction [45]:

$$4NO + 4NH_3 + O_2 \rightarrow 4N_2 + 6H_2O \quad (2)$$

Considering the elemental reactions, the key role of the NH_i radicals in the reduction process becomes evident [42,43]. The ThermalDeNO$_x$ mechanism is well studied, and its dependencies are know [42]: (1) The process has a narrow effective temperature window between 1100 K and 1400 K. (2) Moreover, molecular oxygen must be available. (3) The presence of hydrogen shifts the effective temperature range to lower temperatures. (4) Too high concentrations of NH_3 and water inhibit the reduction process. In the simulations (Fig. 9), during devolatilization and tar break-up at higher temperatures, NH_3 and NO are released to the gas phase. At higher temperatures, the present NH_3 effectively reduces the NO to nitrogen N_2. The reduction process is enhanced with the leaner conditions so that at 1223 K and $\lambda = 0.4$, all NH_3 is consumed. The present hydrogen (Fig. 6), shifts the reduction window to lower temperatures so that the highest NO concentrations are found at 923 K to 973 K. With lower concentrations of hydrogen and ammonia for increasing equivalence ratio, the reduction potential reduces for the lower temperature range.

The NO presence at low temperatures further gives insight into the active NO formation pathways. At these low temperatures, the fuel-NO pathways is the most contributing, while the maximum temperatures are too low to activate the thermal-NO pathway. The contribution from the prompt NO pathway is low, which is in accordance with assumptions in previous literature [43].

Fig. 10 shows the release of NO and its precursors over the analysed surrogates and moisture contents. In this figure, the surrogates are shown with descending fuel-bonded nitrogen content. With higher nitrogen content in the surrogates, higher concentrations of NH_3 and HCN are predicted. Since the simulations in these figures are performed at the same temperature and air feed rate, the reduction potential of NO is comparable. An elevated concentration of NH_3, for example, surrogates 17, 6, 14 and 9, leads to lower NO presence. NO concentrations increase with moisture content. Water presence affects NO in two ways, it inhibits the reduction via NH_3 and its radicals and provides further oxidizer by dissociating that promotes NO formation. Overall, at the considered operating conditions, the level of NO in the producer gas is much lower than that of NH_3 and HCN.

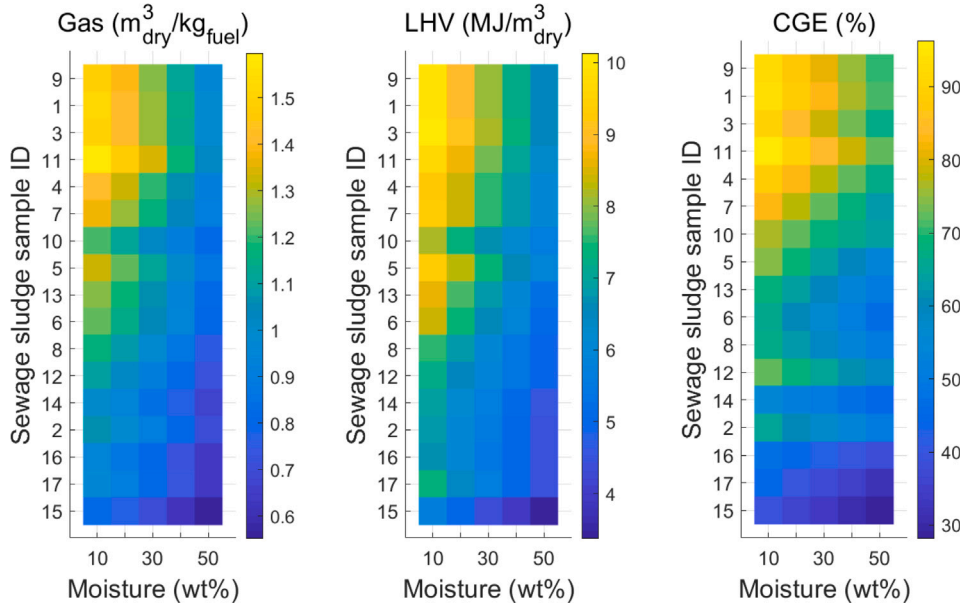

Fig. 8. Prediction of energetic quality over the analysed surrogate compositions and moisture contents. Surrogate samples in descending order after carbon content in the dry ash including surrogate.

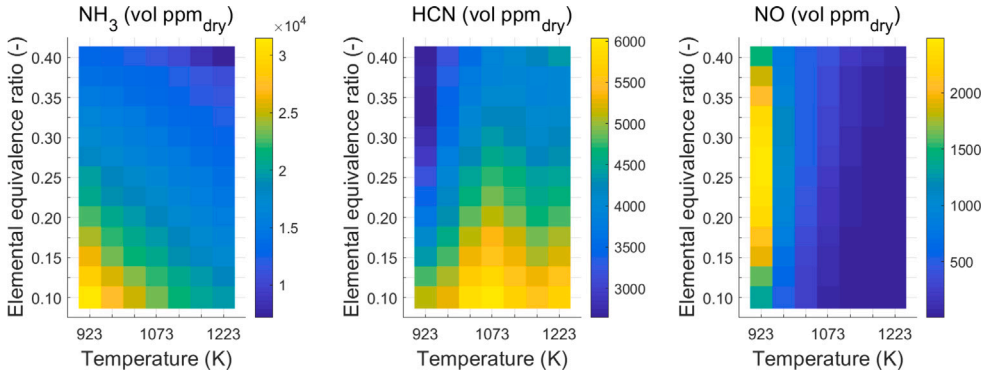

Fig. 9. Prediction of fuel NO and its precursors in the produced gas over the analysed fuel–air ratios and ambient temperatures.

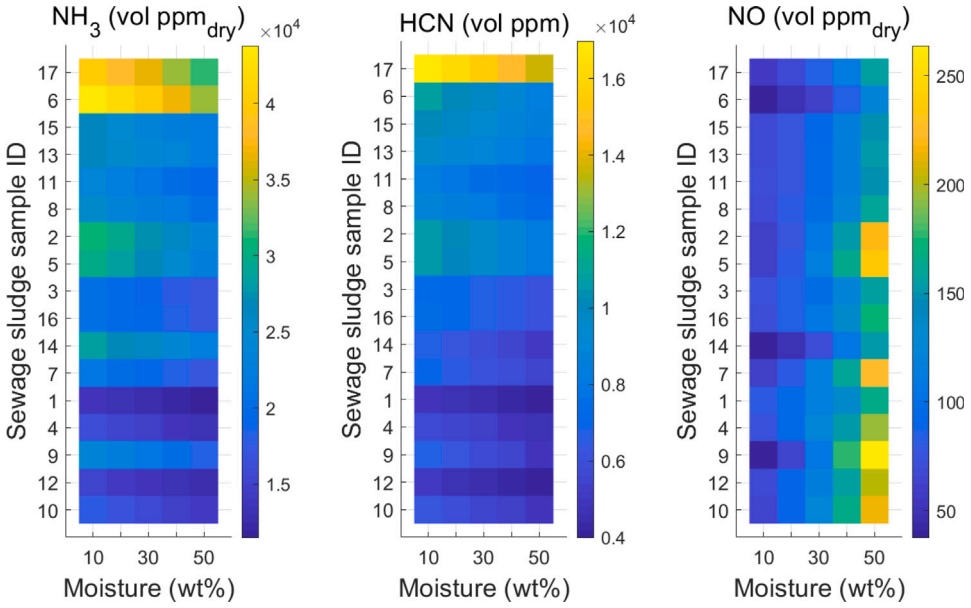

Fig. 10. Prediction of fuel NO and its precursors in the produced gas over the analysed surrogate compositions and moisture contents (bottom row). Surrogates ordered descending after the nitrogen content in the dry ash including composition.

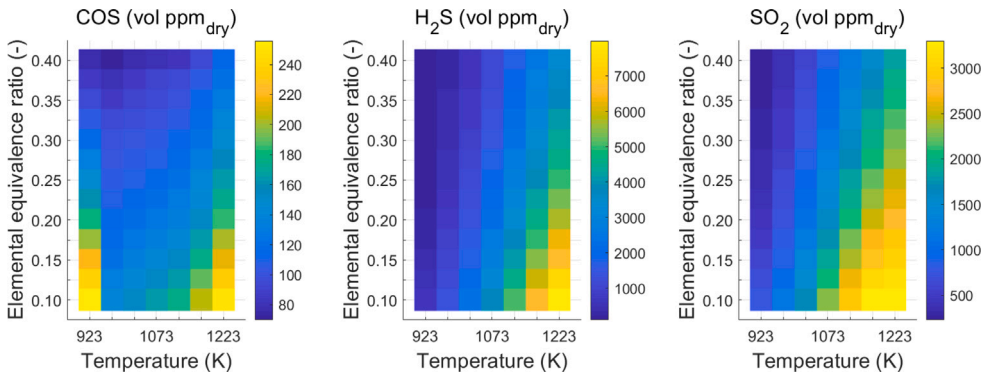

Fig. 11. Prediction of SO_2 and its precursors in the produced gas over the analysed fuel–air ratios and ambient temperatures.

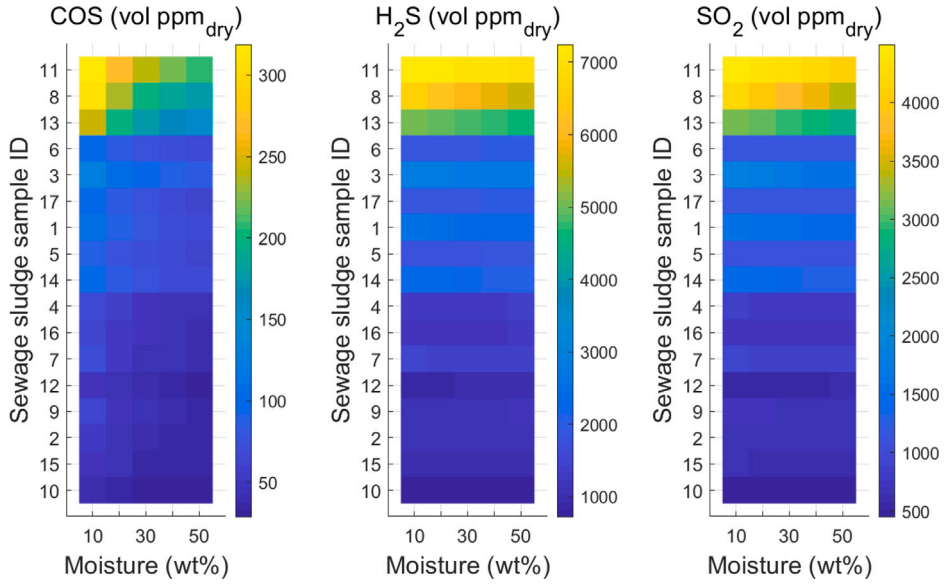

Fig. 12. Prediction of SO_2 and its precursors in the produced gas over the analysed surrogate compositions and moisture contents. Surrogates ordered descending after the sulfur content in the dry ash including composition.

Sulfur is released in the form of three species in the model: carbonyl sulfide COS, hydrogen sulfide H_2S and sulfur dioxide SO_2. Fig. 11 shows their prediction over the temperature and equivalence ratios. Their concentrations in the gas phase are the highest at high temperatures and in rich conditions. Opposite to the considered hydrocarbons and nitrogen species, the model contains no sulfur-containing tar species. Hence, the further decomposition with increased available oxidizer does not increase their composition (compare HCN in Fig. 9). However, the further thermal decomposition of the solid yields more sulfur species. Their concentration is diluted with increasing oxidizer and gas yield (Fig. 8). Carbonyl sulfide COS is released equimolar to hydrogen sulfide H_2S and sulfur dioxide SO_2. Anyhow, the COS concentration in the producer gas is significantly lower. Compared to the other sulfur species, COS is unstable and reacts with oxidizing species to form CO and radicals, such as S and SH. This results in an increased H_2S formation and, at low temperatures, a slight increase in COS concentration due to the high CO concentrations and its inhibiting character as the products of the decomposition reactions. The higher concentration of H_2S than other sulfur species is typically found in biomass and bio-originated waste streams.

Fig. 12 shows the prediction of the main SO_2 and its main precursors over the analysed surrogates of the sludge samples and moisture contents. More sulfur species are released with higher sold-bonded sulfur in the surrogate (Surrogates 11, 8 and 13). The replacement of the dry ash-containing fuel with moisture leads to a lower feed of sulfur to the system and hence a lower concentration of the sulfur species in the gas phase. With decreasing sulfur content in the surrogate, fewer precursors and SO_2 are found in the gases. However, there is no direct connection between the sulfur content and the amount of volatile matter observed for carbon. So, while the absolute amount of sulfur on the mass base decreases from Surrogate 11 to 10, the concentration of the sulfur species varies slightly due to variations in the gas yield.

Even though not in detail discussed in the present work due to their low concentrations, the emission models also include other oxides such as NO_2, N_2O, SO and SO_3. Hence, the detailed information on NO_x, SO_x and their precursors can indicate needed producer gas cleaning units. Furthermore, the detailed producer gas compositions are a valuable input for the analysis of the further use of the producer gas in a subsequent energy recovery stage. The impact of the present nitrogen and sulfur species on the emission formation during incineration is investigated in further analysis by the authors [46].

4. Conclusion

The combination of a detailed chemistry scheme and a stochastic reactor model is used to model the gasification of sewage sludge in a rotary kiln. The varying chemical composition and energy content of sewage sludge is modelled using a surrogate approach. The impact of gasification operation parameters and fuel properties is analysed in

terms of producer gas quality, cold gas efficiency of the process and gas species formation.

It is found that the model well predicts the trends with increasing temperature and air feed rate. The model and presented analysis allow an understanding of the conversion behaviour of the released hydrocarbons and the complex nitrogen chemistry.

The gas composition of the produced gas and hence its lower heating value and the cold gas efficiency of the process are impacted largely by the fuel properties. The highest methane and carbon monoxide compositions are found for dry sludge surrogates with high volatile content and high carbon dioxide formation for wet sludge with low volatile content. The increase of moisture content leads to a reduction in the lower heating value of 30%. The cold gas efficiency varies between sludge samples up to 60%.

The release of nitrogen and sulfur species increases with the content of these elements in the fuel, and high moisture contents lead to a lower formation of the emission precursors.

The generated maps over various operating conditions allow finding the optimum in lower heating value and species concentrations, such as hydrogen H_2 and cold gas efficiency. The results can be used within the design process of gasification plants to account for high efficiency and favourable composition for the targeted further use of the producer gas. The knowledge of the variability with the solid feedstock helps to understand expected maxima and minima in efficiency but also targeted products and emission formation. These details can be used as input during cost estimation and for the design of process control.

Future work will address the calculation of the exergy balance of the processes and the use of the producer gas. Herby, further upgrading of the producer gas and its direct use in incineration will be investigated.

CRediT authorship contribution statement

Corinna Netzer: Conceptualization, Methodology, Software, Formal analysis, Investigation, Visualization, Writing – original draft, Writing – review & editing. **Ning Guo:** Conceptualization, Methodology, Writing – review & editing. **Ivar Ståle Ertesvåg:** Funding acquisition, Writing – review & editing. **Terese Løvås:** Funding acquisition, Writing – review & editing.

Declaration of competing interest

The authors declare the following financial interests/personal relationships which may be considered as potential competing interests: Corinna Netzer reports financial support was provided by Research Council of Norway. Ning Guo reports financial support was provided by National Centre for Research and Development (Poland).

Data availability

Model input and output are provided in an appendix. Other data is available upon request.

Acknowledgements

The research leading to these results has received funding from the Research Council of Norway via the GASPRO project (No. 267916) and the Norway Grants 2014–2021 via the National Centre for Research and Development (Poland) via the project: “Negative CO2 emission gas power plant” - NOR/ POLNORCCS/ NEGATIVE-CO2-PP/ 0009/2019-00, which is co-financed by programme “Applied research” under the Norwegian Financial Mechanisms 2014–2021 POLNOR CCS 2019 - Development of CO2 capture solutions integrated in power and industry processes.

Appendix A. Supplementary data

Supplementary material related to this article can be found online at https://doi.org/10.1016/j.fuel.2022.127297.

References

[1] Tsybina A, Wuensch C. Analysis of sewage sludge thermal treatment methods in the context of circular economy. Detritus 2018;2:3–15. http://dx.doi.org/10.31025/2611-4135/2018.13668.
[2] Adar E, Ince M, Bilgili MS. Supercritical water gasification of sewage sludge by continuous flow tubular reactor: A pilot scale study. Chem Eng J 2020;391:123499. http://dx.doi.org/10.1016/j.cej.2019.123499.
[3] Fytili D, Zabaniotou A. Utilization of sewage sludge in EU application of old and new methods—A review. Renew Sustain Energy Rev 2008;12(1):116–40. http://dx.doi.org/10.1016/j.rser.2006.05.014.
[4] Eriksson E, Christensen N, Ejbye Schmidt J, Ledin A. Potential priority pollutants in sewage sludge. Desalination 2008;226(1):371–88. http://dx.doi.org/10.1016/j.desal.2007.03.019, 10th IWA International Specialized Conference on Diffuse Pollution and Sustainable Basin Management.
[5] Gupta A, Kumar M, Srivastava S. Recent advances in wastewater sludge valorization. In: Shah S, Venkatramanan V, Prasad R, editors. Bio-valorization of waste: Trends and perspectives. Singapore: Springer Singapore; 2021, p. 225–47. http://dx.doi.org/10.1007/978-981-15-9696-4_10.
[6] Montagnaro F, Tregambi C, Salatino P, Senneca O, Solimene R. Modelling oxy-pyrolysis of sewage sludge in a rotary kiln reactor. Fuel 2018;231:468–78. http://dx.doi.org/10.1016/j.fuel.2018.05.094.
[7] Werle S, Sobek S. Gasification of sewage sludge within a circular economy perspective: a Polish case study. Environ Sci Pollut Res 2019;26:35422–32. http://dx.doi.org/10.1007/s11356-019-05897-2.
[8] Gorazda K, Tarko B, Werle S, Wzorek Z. Sewage sludge as a fuel and raw material for phosphorus recovery: Combined process of gasification and P extraction. Waste Manage 2018;73:404–15. http://dx.doi.org/10.1016/j.wasman.2017.10.032.
[9] Gao N, Jia X, Gao G, Ma Z, Quan C, Naqvi SR. Modeling and simulation of coupled pyrolysis and gasification of oily sludge in a rotary kiln. Fuel 2020;279:118152. http://dx.doi.org/10.1016/j.fuel.2020.118152.
[10] Calvo L, García A, Otero M, et al. An experimental investigation of sewage sludge gasification in a fluidized bed reactor. Sci World J 2013;2013:479403. http://dx.doi.org/10.1155/2013/479403.
[11] Manyà JJ, Sánchez JL, Gonzalo A, Arauzo J. Air gasification of dried sewage sludge in a fluidized bed: effect of the operating conditions and in-bed use of alumina. Energy Fuels 2005;19(2):629–36. http://dx.doi.org/10.1021/ef0497614.
[12] Judex JW, Gaiffi M, Burgbacher HC. Gasification of dried sewage sludge: Status of the demonstration and the pilot plant. Waste Manage 2012;32(4):719–23. http://dx.doi.org/10.1016/j.wasman.2011.12.023.
[13] Seggiani M, Vitolo S, Puccini M, Bellini A. Cogasification of sewage sludge in an updraft gasifier. Fuel 2012;93:486–91. http://dx.doi.org/10.1016/j.fuel.2011.08.054.
[14] Dogru M, Midilli A, Howarth CR. Gasification of sewage sludge using a throated downdraft gasifier and uncertainty analysis. Fuel Process Technol 2002;75(1):55–82. http://dx.doi.org/10.1016/S0378-3820(01)00234-X.
[15] Phuphuakrat T, Nipattummakul N, Namioka T, Kerdsuwan S, Yoshikawa K. Characterization of tar content in the syngas produced in a downdraft type fixed bed gasification system from dried sewage sludge. Fuel 2010;89(9):2278–84. http://dx.doi.org/10.1016/j.fuel.2010.01.015.
[16] Freda C, Cornacchia G, Romanelli A, Valerio V, Grieco M. Sewage sludge gasification in a bench scale rotary kiln. Fuel 2018;212:88–94. http://dx.doi.org/10.1016/j.fuel.2017.10.013.
[17] Gikas P. Ultra high temperature gasification of municipal wastewater primary biosolids in a rotary kiln reactor for the production of synthesis gas. J Environ Manag 2017;203:688–94. http://dx.doi.org/10.1016/j.jenvman.2016.02.043.
[18] Peng L, Wang Y, Lei Z, Cheng G. Co-gasification of wet sewage sludge and forestry waste in situ steam agent. Bioresour Technol 2012;114:698–702. http://dx.doi.org/10.1016/j.biortech.2012.03.079.
[19] Chun YN, Kim SC, Yoshikawa K. Pyrolysis gasification of dried sewage sludge in a combined screw and rotary kiln gasifier. Appl Energy 2011;88(4):1105–12. http://dx.doi.org/10.1016/j.apenergy.2010.10.038.
[20] Žnidarčič A, Katrašnik T, Zsély I, Nagy T, Seljak T. Sewage sludge combustion model with reduced chemical kinetics mechanisms. Energy Convers Manage 2021;236:114073. http://dx.doi.org/10.1016/j.enconman.2021.114073.
[21] Debiagi PEA, Pecchi C, Gentile G, Frassoldati A, Cuoci A, Faravelli T, Ranzi E. Extractives extend the applicability of multistep kinetic scheme of biomass pyrolysis. Energy Fuels 2015;29(10):6544–55. http://dx.doi.org/10.1021/acs.energyfuels.5b01753.
[22] Sommariva S, Maffei T, Migliavacca G, Faravelli T, Ranzi E. A predictive multi-step kinetic model of coal devolatilization. Fuel 2010;89(2):318–28. http://dx.doi.org/10.1016/j.fuel.2009.07.023.

[23] Ranzi E, Cuoci A, Faravelli T, Frassoldati A, Migliavacca G, Pierucci S, Sommariva S. Chemical kinetics of biomass pyrolysis. Energy Fuels 2008;22(6):4292–300. http://dx.doi.org/10.1021/ef800551t.
[24] Ranzi E, Pierucci S, Aliprandi P, Stringa S. Comprehensive and detailed kinetic model of a traveling grate combustor of biomass. Energy Fuels 2011;25(9):4195–205. http://dx.doi.org/10.1021/ef200902v.
[25] Anca-Couce A, Mehrabian-Bardar R, Scharler R, Obernberger I. Kinetic scheme of biomass pyrolysis considering secondary charring reactions. Energy Convers Manage 2014;87:687–96. http://dx.doi.org/10.1016/j.enconman.2014.07.061.
[26] Debiagi P, Gentile G, Cuoci A, Frassoldati A, Ranzi E, Faravelli T. A predictive model of biochar formation and characterization. J Anal Appl Pyrolysis 2018;134:326–35. http://dx.doi.org/10.1016/j.jaap.2018.06.022.
[27] Netzer C, Li T, Løvås T. Surrogate reaction mechanism for waste incineration and pollutant formation. Energy Fuels 2021;35(9):7030–49. http://dx.doi.org/10.1021/acs.energyfuels.0c03485.
[28] Netzer C, Løvås T. Chemical model for thermal treatment of sewage sludge. ChemEngineering 2022;6(1). http://dx.doi.org/10.3390/chemengineering6010016.
[29] LOGE AB. LOGEsoft v1.10. 2018, http://www.logesoft.com.
[30] Weber K, Li T, Løvås T, Perlman C, Seidel L, Mauss F. Stochastic reactor modeling of biomass pyrolysis and gasification. J Anal Appl Pyrolysis 2017;124:592–601. http://dx.doi.org/10.1016/j.jaap.2017.01.003.
[31] Francisca Gómez-Rico M, Font R, Fullana A, Martín-Gullón I. Thermogravimetric study of different sewage sludges and their relationship with the nitrogen content. J Anal Appl Pyrolysis 2005;74(1):421–8. http://dx.doi.org/10.1016/j.jaap.2004.11.029, Pyrolysis 2004.
[32] Lumley NP, Ramey DF, Prieto AL, Braun RJ, Cath TY, Porter JM. Techno-economic analysis of wastewater sludge gasification: A decentralized urban perspective. Bioresour Technol 2014;161:385–94. http://dx.doi.org/10.1016/j.biortech.2014.03.040.
[33] Debiagi PEA, Trinchera M, Frassoldati A, Faravelli T, Vinu R, Ranzi E. Algae characterization and multistep pyrolysis mechanism. J Anal Appl Pyrolysis 2017;128:423–36. http://dx.doi.org/10.1016/j.jaap.2017.08.007.
[34] Cuoci A, Faravelli T, Frassoldati A, Granata S, Migliavacca G, Pierucci S, Ranzi E, Sommariva S. A general mathematical model of biomass devolatilization. Note 2. Detailed kinetics of volatile species. In: 30th meeting on combustion, Italian section of the combustion institute. 2007, p. 008.
[35] Glarborg P, Kubel D, Dam-Johansen K, Chiang H-M, Bozzelli JW. Impact of SO2 and NO on CO oxidation under post-flame conditions. Int J Chem Kinet 1996;28(10):773–90. http://dx.doi.org/10.1002/(SICI)1097-4601(1996)28:10<773::AID-KIN8>3.0.CO;2-K.
[36] Glarborg P, Marshall P. Oxidation of reduced sulfur species: Carbonyl sulfide. Int J Chem Kinet 2013;45(7):429–39. http://dx.doi.org/10.1002/kin.20778.
[37] Glarborg P, Miller JA, Ruscic B, Klippenstein SJ. Modeling nitrogen chemistry in combustion. Prog Energy Combust Sci 2018;67:31–68. http://dx.doi.org/10.1016/j.pecs.2018.01.002.
[38] Kraft M, Maigaard P, Mauss F, Christensen M, Johansson B. Investigation of combustion emissions in a homogeneous charge compression injection engine: Measurements and a new computational model. Proc Combust Inst 2000;28(1):1195–201. http://dx.doi.org/10.1016/S0082-0784(00)80330-6.
[39] Netzer C, Li T, Seidel L, Mauß F, Løvås T. Stochastic reactor-based fuel bed model for grate furnaces. Energy Fuels 2020;34(12):16599–612. http://dx.doi.org/10.1021/acs.energyfuels.0c02868.
[40] Channiwala S, Parikh P. A unified correlation for estimating HHV of solid, liquid and gaseous fuels. Fuel 2002;81(8):1051–63. http://dx.doi.org/10.1016/S0016-2361(01)00131-4.
[41] Xiong S, Zhuo J, Zhang B, Yao Q. Effect of moisture content on the characterization of products from the pyrolysis of sewage sludge. J Anal Appl Pyrolysis 2013;104:632–9. http://dx.doi.org/10.1016/j.jaap.2013.05.003.
[42] Miller JA, Bowman CT. Mechanism and modeling of nitrogen chemistry in combustion. Prog Energy Combust Sci 1989;15(4):287–338. http://dx.doi.org/10.1016/0360-1285(89)90017-8.
[43] Glarborg P, Jensen A, Johnsson J. Fuel nitrogen conversion in solid fuel fired systems. Prog Energy Combust Sci 2003;29(2):89–113. http://dx.doi.org/10.1016/S0360-1285(02)00031-X.
[44] Speth K, Murer M, Spliethoff H. Experimental investigation of nitrogen species distribution in wood combustion and their influence on NOx reduction by combining air staging and ammonia injection. Energy Fuels 2016;30(7):5816–24. http://dx.doi.org/10.1021/acs.energyfuels.6b00943.
[45] Duo W, Dam-Johansen K, Østergaard K. Kinetics of the gas-phase reaction between nitric oxide, ammonia and oxygen. Can J Chem Eng 1992;70(5):1014–20. http://dx.doi.org/10.1002/cjce.5450700525.
[46] Guo N, Lewandowski MT, Netzer C. Predictions of NOx and SOx in MILD regime based on thermal conversion of solid sewage sludge surrogates. Fuel 2022. submitted for publication.